UNCLASSIFIED

REPORT DOCUMENTATION PAGE

UNCLASSIFIED

Form Approved
OMB No. 0704-0188

AD-A226 829

2. REPORT DATE	3. REPORT TYPE AND DATES COVERED
8/15/90	October 1, 1989-January 31, 1990

4. TITLE AND SUBTITLE

Unsteady Separation over Maneuvering Bodies (Progress)

5. FUNDING NUMBERS

AFOSR-FINAL
88-0229

(2)

6. AUTHOR(S)

S.F. Shen, T. Wu, Z. Xiao and J.S. Kim

AFOSR-TR- 90 0948

7. PERFORMING ORGANIZATION NAME(S) AND ADDRESS(ES)

Cornell University
Ithaca, NY 14853

8. PERFORMING ORGANIZATION REPORT NUMBER

6110 2F
2307/A3

9. SPONSORING/MONITORING AGENCY NAME(S) AND ADDRESS(ES)

AIR FORCE OFFICE OF SCIENTIFIC RESEARCH
DIRECTORATE OF AEROSPACE SCIENCES
BOLLING AFB, DC 20332-6448

10. SPONSORING/MONITORING AGENCY REPORT NUMBER

DTIC
ELECTE
SEP 26 1990
S D
D CS

11. SUPPLEMENTARY NOTES

12a. DISTRIBUTION/AVAILABILITY STATEMENT

APPROVED FOR PUBLIC RELEASE
DISTRIBUTION IS UNLIMITED

12b. DISTRIBUTION CODE

13. ABSTRACT (Maximum 200 words)

Development of a new boundary layer code has reached the status to permit meaningful applications. Computations have been carried out for the initiation of separation in the symmetry plane of a prolate spheroid of slenderness ratio 1/4, impulsively started into forward motion at zero incidence and also at 50 degrees angle. This case serves as validation by comparing with previously published results of Xu and Wang (ref.1), and also demonstrates that our method gives information of flow near the rear stagnation point not available in the literature. More studies have been performed on the optimization of surface suction to delay or prevent the unsteady separation for an impulsively started circular cylinder. Here the methodology should be of interest. Work on an unsteady three-dimensional thin-layer Navier-Stokes code, however, is progressing slowly.

14. SUBJECT TERMS

Unsteady separation, three-dimensional moving body, separation control

15. NUMBER OF PAGES

20

16. PRICE CODE

17. SECURITY CLASSIFICATION OF REPORT	18. SECURITY CLASSIFICATION OF THIS PAGE	19. SECURITY CLASSIFICATION OF ABSTRACT	20. LIMITATION OF ABSTRACT
UNCLASSIFIED	UNCLASSIFIED	UNCLASSIFIED	

NSN 7540-01-280-5500

Standard Form 298 (Rev. 2-89)
Prescribed by ANSI Std. Z39-18

UNCLASSIFIED

DTIC FILE COPY

Technical Rept for AFOSR 88-0229, for the period Oct. '89 to Feb. '90

by S.F. Shen, Cornell University

We have reached the termination date of the Grant 88- 0229, except for a new minimal extension to enable us to bring our major effort, Wu's study of the unsteady separation process on a three-dimensional body, to at least some concrete conclusion by the end of August, 1990. While we are grateful for Capt. Helin's sustained interest in our project, the amount available to us from AFOSR will not cover half the cost. We shall try to manage with forced reductions of expenditure in the last few months and the principal investigator is taking zero compensation.

The progress of the project between Oct. '89 and Feb. '90 in all three active studies outlined in the last Technical Report (Oct. '89) is summarized as follows. They consist of:

1) Three-dimensional unsteady separation over an impulsively started prolate spheroid, at zero and also 50 degrees of angle of attack;

2) Feasibility study of controlling two-dimensional unsteady separation over a circular cylinder by surface suction;

3) Development of an unsteady thin-layer ('parabolized') Navier-Stokes code for boundary-layer behavior subsequent to the initiation of separation.

Project 1) has been carried out by T.Wu. During this period the focus has been a NEW three-dimensional unsteady boundary-layer Eulerian code for flow in the symmetrical plane. After careful validation it is now in operational form. The first application was to recalculate the case in the published work of Xu and Wang (ref. 1), having to do with the process leading to initial separation in the plane of symmetry. Our procedure in principle has two major advantages: the multizone formulation eliminates the difficulty associated with the geometrical singularity, and the initial-value approach allows accurate treatment of the moving stagnation points. A paper has been prepared for presentation at the International Symposium on Nonsteady Flows at the joint ASME and CSME (Canadian) meeting, June '90 in Toronto, Ont. A copy is attached as Appendix A.

Project 2) has been the assignment of Z. Xiao. The basic idea is to exploit our time-accurate Eulerian unsteady boundary-layer code, to study the effects on the initiation of unsteady separation due to various parameters related to the variable motion, as well as the boundary conditions that may suggest strategies for separation control. The Eulerian code must be able to locate incipient separation that has been made clear by our persistent demonstration via the Lagrangian interpretation. In the Eulerian description, most experts now generally agree that the precursor, or signature, of imminent separation is a locally very sharp 'spike' in the displacement thickness. We first establish that in the bench-mark case of an impulsively started circular cylinder, the van Dommelen and Shen (ref.2) solution, recast as the displacement thickness along the wall, is indeed duplicated by our new Eulerian code. Preliminary results have been obtained on the efficacy of delaying or eliminating the occurrence of the 'spike', hence separation, with the application of various surface suction arrangements. These were included in an invited presentation, by S.F.Shen, at the Workshop on Analytical Methods in Unsteady Separation, sponsored by Army ARO, January '90, Columbus OH. A copy of the handout of the talk was submitted with our Technical Report for Oct. '89.

We hope for more results on optimization of controlling unsteady separation before his departure. Because of the budget limitation, however, Mr. Xiao's association with AFOSR-sponsored research will be terminated no later than March 1, 1990.

Project 3) has occupied the attention of Dr. J. S.Kim since his arrival from S. Korea in may '89. As described in earlier Technical Reports, Dr. Kim's attack follows his previous experiences with the Navier-Stokes solver. To rewrite some of the program for use in the Cornell Supercomputer facility proved to be quite time consuming, esp. for applications targeted for three-dimensional bodies. Considerable debugging efforts have been necessary during the present period, and so far the test trials involve only simple geometry and small numbers of time steps. As Dr. Kim is obligated to return to Korea on April 1, 1990, and no funding for possible replacement, it seems unrealistic to expect the final achievement of this work to be more than preliminary exploration. A description of Kim's work can be found in Appendix B.

With regard to publication and presentation, the paper by Shen and Wu (AIAA Paper 88- 3542) is now 'in the press' of the AIAA Journal, after a prolonged unfortunate status as a 'missing manuscript' in the editor's office. In January S.F.Shen gave a colloquium on 'Unsteady Boundary Separation from the Lagrangian View' at the University of Arizona, Tuscon, AZ, followed by the invited talk of the same title (but somewhat different content, including some of the separation control results) at the Columbus Workshop. Wu's results to-date will be presented at the ASME meeting in Toronto this June, already mentioned above.

References

1. Xu ,W.C. and K.C.Wang, "Unsteady Laminar Boundary Layer along the Symmetry Plane of a Prolate Spheroid', J. Fluid Mech., v. 195, 1988, 413-435.

2. Van Dommelen, L.L. and S.F.Shen, "The Spontaneous Generation of the Singularity in a Separating Boundary Layer", J. Comp. Phys., v.38, 1980, 125-140.

Appendices

A. Manuscript of Toronto paper by Wu and Shen.

B. Code Development for the Unsteady Thin Layer Navier-Stokes.

Appendix A
TR 0229, 2/90

A MULTI-ZONE TIME-MARCHING TECHNIQUE FOR UNSTEADY SEPARATING THREE-DIMENSIONAL BOUNDARY-LAYERS AND ITS APPLICATION TO THE SYMMETRY-PLANE SOLUTION OF AN IMPULSIVELY-STARTED PROLATE SPHEROID

Tzuyin Wu* and Shan-Fu Shen**
Sibley School of Mechanical and Aerospace Engineering
Cornell University
Ithaca, New York, 14853

ABSTRACT

Recent interest in unsteady separation and separated flows brings up the need of an accurate and efficient computational scheme for general unsteady three-dimensional boundary-layer flows. Resolution of the singular behavior at separation is a delicate problem. The task is further complicated by the geometrical singularity and the non-stationary stagnation point. The present paper proposes a numerical scheme to sidestep these difficulties. As the first stage of development, the simpler problem of the symmetry-plane solution of the laminar boundary-layer over an impulsively started prolate spheroid is calculated. Results show that the present Eulerian calculation satisfactorily captures the singular behavior of the boundary-layer when separation is approached. Comparison with Xu and Wang's recent results and those for the two-dimensional elliptic cylinder calculated by the Lagrangian method are also made. Discussions of the results for unsteady separation at zero, small and large incidences are presented.

NOMENCLATURE

D_1, D_2	mapping constants in β-direction
e	eccentricity of spheroid
h_1, h_2, h_3	metric coefficients
p	pressure
S	transformed coordinate defined in equation (4)
t	time
t/c	thickness ratio
u	velocity component in x-direction
U_e	value of u at edge of boundary-layer
v	velocity component in y-direction
V_e	value of v at edge of boundary-layer
v_y	derivative of v in y-direction
V_{ye}	value of v_y at edge of boundary-layer
V_o, V_{90}	constants in the velocity distribution at edge of boundary-layer
w	velocity component in z-direction
x	streamwise coordinate along the major axis of prolate spheroid
y	circumferential coordinate
z	boundary-layer coordinate normal to x and y direction
$\hat{\alpha}$	angle of attack
α, β	computational coordinates
δ	difference operator in finite-difference equations
Δ	indicating difference; also, displacement thickness
ε	stretching factor of the mapping in α-direction
μ	average operator in finite-difference equations
ρ	density
τ	wall shear

Subscripts

o	stagnation
s	separation
x,y,z	components in x, y and z directions respectively
,	indicating derivatives

Superscripts

n	n^{th} time level in finite-difference equations
$\bar{()}$	quantities in nose region
$\tilde{()}$	quantities in tail region

* Graduate Research Assistant

** John Edson Sweet Professor of Engineering

INTRODUCTION

The separation of three-dimensional laminar boundary-layer has long been an intriguing subject of both basic and practical interest. Even in the steady case, the separation "pattern" on the body surface, as observed in the experiments, takes a variety of forms. Recent progress in the qualitative theory and the actual computations have greatly improved our understanding of the complex phenomena ([1-11]). In the steady flow, zero wall shear signifies separation and the breakdown of the boundary-layer equation. The usual analysis of steady separation is to focus on the limiting streamlines at the wall. For the unsteady case, it is now well-known that separation starts "off" the wall and neither the wall shear nor the wall streamlines can serve as reliable indicators of separation. But very little is known about the details of the phenomenon. Even numerical examples are hard to come by, since efficient and reliable computational schemes for calculating the general unsteady three-dimensional boundary-layer flow still are not well developed.

In steady flow, the separation of the boundary-layer over a prolate spheroid at various incidence angles has been the subject of several computational studies due to Wang ([6-8], [12-14]). Two different types of separation, "open" and "closed", based on the wall limiting streamlines analysis are proposed. In his terminology, the convergence of the limiting streamlines defines the separation line on the body. At small incidence, a "closed" type separation prevails where the separation line completely separates the limiting streamlines originating from different stagnation points. At moderate incidence, the separation line is approached on two sides by limiting streamlines originating from the same stagnation point. This type of separation is

then classified as "open" separation, since two separation lines, one on each side of the spheroid are formed and are not connected on the lee-side symmetry plane. In a recent paper of Xu and Wang [15], the evolution of the skin friction on the symmetry plane of an impulsively started spheroid is studied. They suggest an unsteady analogy of the above "open" and "closed" separations, the term "separation" used in their study referring to vanishing skin friction in the streamwise direction. An off-symmetry-plane calculation of the above problem has been performed by Ragab [16]. Focus of his work is on the crosswise separation at high incidence. The computational domain covers only the front quarter of the prolate spheroid. His results of skin friction lines support the "open" type separation advocated by Wang for unsteady three-dimensional flows. Following van Dommelen and Shen [17, 18], unsteady boundary-layer separation is better defined by the termination of the boundary-layer solution in a singularity. In the two-dimensional problem, the occurrence of a singularity and its structure have been well established (e.g. [17-20]). In the three-dimensional case, this singularity may form a curve whose projection on the wall can then be properly defined as the "separation line" (Shen [21]). The concept is consistent with that of van Dommelen and Cowley [22], in which the authors examine the asymptotic structure of the unsteady three-dimensional separation in a Lagrangian coordinates system. In fact, the structure of separation is found to be quasi two-dimensional.

Confirmation of this singularity at separation was not part of Xu and Wang's calculation, but is the focal point of the present paper. In order to do so, the numerical scheme has been modified. It is noticed, for instance, that no details of the flow near the trailing edge were included in their results. As pointed out in Cebeci et al. ([10], [11], [23]), a "geometrical singularity" is present at both ends of the prolate spheroid when a body-oriented coordinates system is used. In Xu and Wang [15], no provision was made for the singularities, and their method might lead to local difficulty and inaccuracy, particularly for a slender spheroid. Another problem of the space-marching schemes usually adopted in solving a boundary-layer type equation is associated with the stability consideration. In the unsteady case, the grid size in the reversed flow region is limited by the domain-of-dependence rule (CFL criterion). In particular, the restriction on the time step can become so stringent that the calculation is practically prevented from proceeding further [24]. Still another technical difficulty of the space-marching method is the requirement of a starting profile to initiate the spatial integration. This is not available in the general case involving arbitrary body motion for which the stagnation point is non-stationary.

The present paper is actually the first phase of a more ambitious research program dealing with general three-dimensional unsteady separation over an arbitrarily moving body. In developing a solution scheme, we abandon the conventional space-marching technique and choose instead a more classical initial-value approach. That is, the solution is advanced in the time direction only. This allows the calculation of more general unsteady flows as it does not require a fixed stagnation point to construct the flow downstream. In conjunction with an implicit time-marching scheme, a flow dependent, one-sided spatial difference is applied to discretize the convection terms in accordance with the CFL criterion. The severe restriction on the time step is thus relieved. Finally, to overcome the difficulty of the aforementioned "geometrical singularity", we propose a multi-domain attack. Suitable transformation which removes the singularity is applied at both front and tail regions. Calculations are performed separately in each region, and the solutions are patched on the interfaces by interpolation procedure.

For an orderly development, we limit ourselves first to redo the case of a prolate spheroid, following Xu and Wang [15]. The following presents mainly the boundary-layer development in the symmetrical plane of an impulsively-started prolate spheroid. The governing equations and the relevant coordinates transformation are given in the next section. Details of the numerical scheme and the solution procedure are also described. Calculations are performed for three different angles of attack : 0^0, 6^0 and 50^0. Comparison with Xu and Wang [15] are made. In addition, the results are compared with those for the two-dimensional elliptic cylinder calculated by the Lagrangian method. The significance of the findings of the first occurrence of three-dimensional separation on the lee-side and wind-side, at small and large angles of incidence are discussed. If and when and how different unsteady three-dimensional separation patterns are generated and developed can only be answered by computation of the flow off the symmetry plane. Much more remains to be done.

FORMULATION OF THE PROBLEM

The geometry and the boundary-layer coordinate system of a prolate spheroid, following Xu and Wang [15], are specified in Fig.1. The metric coefficients h_1, h_2 and h_3 are defined as

$$h_1 = \sqrt{\frac{1-e^2x^2}{1-x^2}}, \quad h_2 = \sqrt{(1-e^2)(1-x^2)}, \quad h_3 = 1 ; \quad e = \sqrt{1-(t/c)^2}$$

where t/c denotes the ratio of minor to major axis (axes ratio). After a proper scaling with the free stream velocity and the half-chord length of the prolate spheroid, the non-dimensional forms of the boundary-layer equations on the symmetry plane are, in conventional notation,

$$h_2 \frac{\partial u}{\partial x} + h_1 v_y + h_1 h_2 \frac{\partial w}{\partial z} + u \frac{\partial h_2}{\partial x} = 0 \qquad (1)$$

$$\frac{\partial u}{\partial t} + \frac{u}{h_1}\frac{\partial u}{\partial x} + w\frac{\partial u}{\partial z} = \frac{-1}{\rho h_1}\frac{\partial p}{\partial x} + \frac{\partial^2 u}{\partial z^2} \qquad (2)$$

Crosswise momentum equation is identically zero on the symmetry plane. A supplementary equation can be obtained by differentiating it with respect to the circumferential coordinate y :

$$\frac{\partial v_y}{\partial t} + \frac{u}{h_1}\frac{\partial v_y}{\partial x} + w\frac{\partial v_y}{\partial z} + \frac{v_y^2}{h_2} + \frac{uv_y}{h_1 h_2}\frac{\partial h_2}{\partial x} = \frac{-1}{\rho h_2}\frac{\partial^2 p}{\partial y^2} + \frac{\partial^2 v_y}{\partial z^2} \qquad (3)$$

where v_y stands for $\partial v/\partial y$. Based on the velocity profiles u and v_y, the skin friction and the displacement thickness are defined by

$$\tau_x = \left(\frac{\partial u}{\partial z}\right)_{z=0}, \qquad \tau_{y,y} = \left(\frac{\partial v_y}{\partial z}\right)_{z=0}, \qquad \Delta_x = \int_0^\infty \left(1-\frac{u}{U_e}\right) dz.$$

The above governing equations are then subject to a Rayleigh type initial condition for an impulsively-started motion. As usual, no slip boundary conditions are imposed on the wall, and the velocities at the outer edge of the boundary-layer must approach the values specified by the inviscid potential flow :

$$u = v_y = 0 \quad \text{at } z = 0$$

$$u = U_e = \frac{1}{(1-e^2x^2)^{1/2}}\left[V_0(1-x^2)^{1/2}\cos\hat{\alpha} + V_{90}\frac{t}{c}\, x \sin\hat{\alpha}\cos y \right]$$

$$v_y = V_{ye} = V_{90}\sin\hat{\alpha}\cos y \qquad \text{at } z = \infty$$

where $\hat{\alpha}$ = angle of attack,

$$V_0 = \frac{e^2}{1 - \frac{1-e^2}{2e}\ln\frac{1+e}{1-e}}, \qquad V_{90} = \frac{2V_0}{2V_0 - 1}$$

As already mentioned in the introduction, a difficulty of the present spherical coordinates system is that the metric coefficients h_1, h_2 become singular at both x=-1 and x=+1. A transformation which removes this geometric singularity was proposed by Cebeci et al. [10], [23]. Define

$$\frac{dS}{S} = \frac{h_1 dx}{h_2} = \frac{\sqrt{1-e^2x^2}}{\sqrt{1-e^2}\,(1-x^2)}\,dx \qquad \text{with } S=0 \text{ at } x=-1$$

it follows

$$\bar{S} = B\exp\left[\frac{e}{\sqrt{1-e^2}}\sin^{-1}(ex)+A\right]\left[\frac{\sqrt{1-e^2}\sqrt{1-e^2x^2}-e^2x+1}{\sqrt{1-e^2}\sqrt{1-e^2x^2}+e^2x+1}\right]^{1/2}\sqrt{\frac{1+x}{1-x}} \quad (4)$$

where A and B are mapping constants. With transformation (4), and further let

$$\bar{x} = \bar{S}\cos y \qquad u = \bar{u}\cos y + \bar{v}\sin y$$
$$\bar{y} = \bar{S}\sin y \qquad v = -\bar{u}\sin y + \bar{v}\cos y$$
$$\bar{z} = z \qquad w = \bar{w}$$

Equations (1), (2) and (3) then become

$$\frac{1}{\bar{h}}\left(\frac{\partial \bar{u}}{\partial \bar{x}} + \bar{v}_{\bar{y}}\right) + \frac{\partial \bar{w}}{\partial \bar{z}} - \bar{R}\bar{x}\bar{u} = 0 \quad (5)$$

$$\frac{\partial \bar{u}}{\partial t} + \frac{\bar{u}}{\bar{h}}\frac{\partial \bar{u}}{\partial \bar{x}} + \bar{w}\frac{\partial \bar{u}}{\partial \bar{z}} = \frac{-1}{\rho\bar{h}}\frac{\partial p}{\partial \bar{x}} + \frac{\partial^2 \bar{u}}{\partial \bar{z}^2} \quad (6)$$

$$\frac{\partial \bar{v}_{\bar{y}}}{\partial t} + \frac{1}{\bar{h}}\left(\bar{u}\frac{\partial \bar{v}_{\bar{y}}}{\partial \bar{x}} + \bar{v}_{\bar{y}}^2\right) + \bar{w}\frac{\partial \bar{v}_{\bar{y}}}{\partial \bar{z}} - \bar{R}\bar{u}\left(\bar{x}\bar{v}_{\bar{y}} - \bar{u}\right) = \frac{-1}{\rho\bar{h}}\frac{\partial^2 p}{\partial \bar{y}^2} + \frac{\partial^2 \bar{v}_{\bar{y}}}{\partial \bar{z}^2} \quad (7)$$

where $\bar{h} = \frac{h_2}{\bar{S}}$, $\bar{R} = \frac{1}{\bar{S}}\left(\frac{1}{h_2} - \frac{1}{h_1 h_2}\frac{\partial h_2}{\partial x}\right)$

Equations (5), (6), and (7) are now regular at x=-1. Similar treatment can be applied to remove the singularity at the rear end x=+1 and we shall not restate the derivation here. In the following context, quantities in the transformed coordinates near the trailing edge of the prolate spheroid will be denoted by $(\bar{\ })$.

SOLUTION METHOD

The solution domain is decomposed into four regions as shown in Fig.2. The transformed coordinate system described in the last section is used in the nose and tail regions to remove the geometry singularity. Each region is overlapped with the adjacent ones. Calculations are performed separately in different regions, the required boundary conditions on the interface of one region are then obtained from interpolating the values at the interior points of the other region. Successful results where similar composite-grid techniques have been applied were reported in several previous investigations of Navier-Stokes flows ([25], [26]), transonic flows ([27], [28], [29]), Euler equations ([29], [30]), and the combined Navier-Stokes, Euler and boundary-layer equations [31]. The principal advantages of composite-grid are the generation of grids for regions of complicated geometry, and an easier implementation of different formulations in different regions. However, the "patching" of the solutions between different regions needs attention. Care must be taken so that the interpolation procedure on the interface will not destroy the stability and accuracy of the interior solution. See, e.g. Chesshire and Henshaw [25]. In the following calculations, a cubic Lagrangian interpolation formula was used. No apparent error and instability were observed in this particular numerical example.

The physical domain is more conveniently transformed into a finite computational region (α,β) by using appropriate mapping functions. In the main region, for example,

$$x = (x_2-x_1)\left[(1-\varepsilon)(3-2\alpha)\alpha^2 + \varepsilon\alpha\right] + x_1 \qquad 0 \le \alpha \le 1$$

$$z = D_2\sqrt{\frac{t}{t+D_1}}\tan\frac{\pi\beta}{2} \qquad 0 \le \beta \le 1$$

where x_1, x_2 and D_1, D_2 are constants, ε is a small number which controls the stretching in the streamwise coordinate x. The mapping in the α-direction gives the mesh clustering effect near the leading and trailing edges where the pressure gradient varies rapidly. The time-like β coordinate removes the singular behavior in the flow at impulsive start-up. A uniform grid is drawn in the α-β plane, and the governing equations are discretized in terms of these computational coordinates.

In contrast to the conventional space-marching technique in solving the boundary-layer type equation, we next formulate strictly an initial-value problem in which the flow variables in each region are advanced in the time-direction only. A similar approach was already carried out in Van Dalsem and Steger [32] who used a time-relaxation scheme in their calculations. We seek to reduce the computation effort at each time step by adopting a non-iterative predictor-corrector formulation, Douglas [33]. That is, in advancing the time step from n to n+1, a predicted value is first evaluated at n+1/2 where all the non-linear coefficients in the momentum equations are linearized by using the values frozen from the previous time n. Thus the governing equations are decoupled in the predictor step. A backward Euler differencing in time is preferred in solving the predictor value for the purpose of damping out the numerical error. Second order accuracy of temporal difference can be restored by following a Crank-Nicolson like correction step.

In both the predictor and the corrector steps, a flow dependent, one-sided spatial difference is applied to the convection term in accordance with its hyperbolic character (backward difference if u>0 and forward difference for u<0). Unlike the usual marching scheme where flow quantities needed to account for the backflow influence are grabbed from the previous time level. By appealing to the CFL criterion, this explicit formulation will then restrain the time step used in the discretization procedure. This is particularly important as the restriction on the step size can be very stringent when separation is approached [24]. In the present scheme, an implicit time-advancing approach is used, and upwind differences are performed at the current time level throughout the whole domain. The CFL condition is satisfied automatically, allowing us to relax the time-step limitation.

The formulation is very similar in both the predictor and corrector steps. By applying the above discretization procedures to (2) and (3), the following are the resulting finite difference equations in the computational plane-(α,β) for the corrector step :

$$\left\{1+\frac{\Delta t\,\alpha_{,x}u}{2h_1\Delta\alpha}\delta_\alpha^{\pm} - \frac{\Delta t\,\beta_{,z}^2}{2\Delta\beta^2}\delta_\beta^2 - \frac{\Delta t(\beta_{,zz}-\beta_{,t}\beta_{,z}w)}{4\Delta\beta}(2\mu\delta)_\beta\right\}^{n+1/2}\Delta q^{n+1} =$$

$$\frac{-\Delta t}{\rho h_1}\frac{\partial p}{\partial x} + \Delta t\left\{\frac{-\alpha_{,x}u}{h_1\Delta\alpha}\delta_\alpha^{\pm} - \frac{\beta_{,z}^2}{\Delta\beta^2}\delta_\beta^2 - \frac{(\beta_{,zz}-\beta_{,t}\beta_{,z}w)}{2\Delta\beta}(2\mu\delta)_\beta\right\}^{n+1/2}u^n \quad (8)$$

$$\left\{1+\frac{\Delta t\,\alpha_{,x}u}{2h_1\Delta\alpha}\delta_\alpha^{\pm} - \frac{\Delta t\,\beta_{,z}^2}{2\Delta\beta^2}\delta_\beta^2 - \frac{\Delta t(\beta_{,zz}-\beta_{,t}\beta_{,z}w)}{4\Delta\beta}(2\mu\delta)_\beta\right\}^{n+1/2}\Delta q_y^{n+1} =$$

$$\frac{-\Delta t}{\rho h_2}\frac{\partial^2 p}{\partial y^2} - \frac{\Delta t(v_y^2)^{n+1/2}}{h_2} - \frac{\Delta t\,u^{n+1/2}v_y^{n+1/2}}{h_1 h_2}\frac{\partial h_2}{\partial x} +$$

$$\Delta t\left\{\frac{-\alpha_{,x}u}{h_1\Delta\alpha}\delta_\alpha^{\pm} - \frac{\beta_{,z}^2}{\Delta\beta^2}\delta_\beta^2 - \frac{(\beta_{,zz}-\beta_{,t}\beta_{,z}w)}{2\Delta\beta}(2\mu\delta)_\beta\right\}^{n+1/2}v_y^n \quad (9)$$

where $\Delta q^{n+1} = u^{n+1} - u^n$

$$\Delta q_y^{n+1} = v_y^{n+1} - v_y^n$$

$\alpha_{,x}$, $\beta_{,t}$, $\beta_{,z}$ and $\beta_{,zz}$ denote the derivatives of the corresponding mapping functions. The difference operators used [illegible] defined in Warming and Beam [34] :

$$\delta = (\cdot)_{i+1/2} - (\cdot)_{i-1/2} \qquad \delta^+ = (\cdot)_{i+1} - (\cdot)_i \qquad \delta^- = (\cdot)_i - (\cdot)_{i-1}$$

$$\delta^2 = (\cdot)_{i+1} - 2(\cdot)_i + (\cdot)_{i-1} \qquad \mu = 1/2\left[(\cdot)_{i+1/2} + (\cdot)_{i-1/2}\right]$$

Equations (8) and (9) are then factored into two sweeps by the approximate factorization procedure of Warming and Beam [34]. Each sweep involves solving a system of algebraic equations with a scalar tri-diagonal coefficient matrix :

$$\left(1 - \frac{\Delta t\, \beta_{,z}^2}{2\Delta\beta^2}\delta_\beta^2 - \frac{\Delta t(\beta_{,zz}-\beta_{,t}-\beta_{,z}w)}{4\Delta\beta}(2\mu\delta)_\beta\right)^{n+1/2}\Delta\tilde{q}^{n+1} = \text{RHS of (8)}$$

$$\left(1 + \frac{\Delta t\, \alpha_{,x}u}{2h_1\Delta\alpha}\delta_\alpha^{\mp}\right)^{n+1/2}\Delta q^{n+1} = \Delta\tilde{q}^{n+1}$$

Having solved u and v_y, the transverse velocity w can be updated from integrating the continuity equation (1) by trapezoidal rule.

Similar difference schemes are applied to the equations in the transformed coordinates systems for the nose and tail regions. Their final forms are omitted here for brevity.

The accuracy of the predictor-corrector method used has been studied by Douglas [33] on 1-D model equations. The results show that for a transient problem, the overall accuracy in time is of second order. Linearized von Neumann stability analysis of the corrector step predicts the scheme to be unconditionally stable if the one-side difference conforms with the flow direction. In the following numerical examples, no instability was encountered in the calculations. Furthermore, in order to preserve second order accuracy in the spatial direction, the convection terms were discretized by a three-point upwind difference formula. This will result in a penta-diagonal matrix in the α-sweep rather than tri-diagonal during the factorization procedure. Both matrices were solved using well vectorized penta- and tri-diagonal solvers.

RESULTS AND DISCUSSION

Calculations were done for the symmetry plane of a prolate spheroid with axes ratio 1/4 and various angles of attack which typify the axisymmetry (0^o), low incidence (6^o) and high incidence (50^o) categories. To assure the convergence of the solution, a numerical test on the effects of grid refinement was performed first and the results are included in the appendix. At each different incidence, the skin friction and displacement thickness are presented and discussed in the following subsections. The focus will be on the initiation of separation evidenced by the emergence of a Lagrangian singularity in the flow. Because of the similarity between the flow in the symmetry plane and the two-dimensional cylinder case, comparison with the results obtained from the two-dimensional elliptic cylinder with the same axes ratio is made, and certain analogy between the two flows is shown.

All the numerical computations were performed on the Cornell National Supercomputer Facility. For a typical 30,000 grid points (including all four regions) used in each of the present examples, the required CPU time in advancing one time step was around 2 seconds on IBM 3090-600E. About 45% of the job was executed under the vector mode, and the measured vector speed-up was 3. More effort is being made to improve the percentage of vectorization of the program.

0^o Incidence

The zero degree incidence case was not included in Xu and Wang's calculation [15]. It is given here as a bench test of the present numerical scheme. Calculated wall shear and displacement thickness are shown in Figs.3 to 8. In the nose region, the skin friction $\tilde{\tau}_{\tilde{x}}$ quickly approaches a steady value (Fig.3) while in the tail region, Fig.4, a reversed-flow region is seen to form shortly after the impulsive start and spread subsequently toward the leading edge. Also notice that due to the small axes ratio, the reversed flow is confined in a narrow region near the trailing edge, and the skin friction does not vary much along most part of the body (Fig.5). Figure 6 plots the distribution of crosswise skin friction $\tau_{y,y}$. Owing to the axisymmetry property of the flow at 0^o incidence, the value of $\tau_{y,y}$ is zero in this particular case. However, as pointed out in the previous section, quantities on the left and right interfaces of the main region are obtained from interpolating the flow variables in the nose and tail regions respectively. Specifically, the crosswise skin friction in the main region is related to that in the nose through the transformation

$$\tau_{y,y} = -\tilde{\tau}_{\tilde{x}}\cos y + \tilde{\tau}_{\tilde{y},\tilde{y}}\tilde{S}\cos^2 y.$$

In general, terms on the right hand side of the above transformation do not sum up to zero due to discretization and hence introducing error on the interface. It can be seen from Fig.6 that this error on the left interface is quickly damped out after a few nodal points, while the error on the downstream interface does not propagate back into the domain because of the upwind differencing. The accuracy of the solution at the interior points is found to be essentially unaffected.

The displacement thickness $\Delta_{\tilde{x}}$ is given in Fig.7 and Fig.8. In the main region (Fig.7), the flow changes slowly over a large part of the body except very close to the trailing edge where the boundary-layer increases drastically. Figure 8 shows the details just ahead of the trailing edge. A "spike"-like structure similar to that discovered in the Lagrangian computations of two-dimensional problems ([17], [18], [35]) is observed near $\tilde{x}$=-0.08. In order to be convinced that it is not created by numerical instability, the calculation was carried out again in several refined meshes and reduced time steps. Results show only a "sharper" spike and the overall picture does not change. Formerly, this "spike"-like behavior has only been found in Lagrangian computations. Most of the previous two-dimensional boundary-layer results calculated by the Eulerian formulation encountered difficulty near "separation" and consequently did not give a conclusive displacement thickness variation at this point (e.g. [36-39]). Failure to obtain a converged and stable solution in these calculations upon approaching separation may be attributed to the aforementioned severe limitation on the step size needed in the conventional space-marching technique. The present time-marching Eulerian scheme proves to be not only stable but also capable of confirming the critical features near separation which were previously obtained by the Lagrangian computation.

The behavior of the displacement thickness reflects the behavior of the velocity profile $\tilde{u}$. Shown in Fig.9 is the velocity profile at several $\tilde{x}$ locations. It is found that starting from t=0.19, there is an unusual "clustering" of the velocity profiles around $\tilde{x}$=-0.045. The same phenomenon was reported in Cebeci [36]. The clustering of the velocity profiles results in a "kink" in the $\tilde{\Delta}_{\tilde{x}}$ distribution at t=0.20, Fig.8. Beyond t=0.20, there is a sudden thickening in some of the velocity profiles (Figs.9b, c) which in turn leads to a fast increase in the displacement thickness at such locations. The peculiar velocity profiles are only found to occur in a very narrow region of $\tilde{x}$. Further into the reversed flow regime, the velocity profiles look normal again. The formation of the sharp "spike" and the "valley" immediately following in the displacement thicknesses for t>0.20, Fig.8, are thus explained.

Accompanying this thickening of the displacement thickness is the sudden growth in the transverse velocity $\tilde{w}$. From the Lagrangian view point ([18], [40]), the thickening happens because a certain fluid "packet" gets squeezed in the streamwise direction and must expand laterally in order to preserve the volume. Since in the axisymmetry case every meridian plane that cuts through the prolate spheroid is a symmetry plane, the critical fluid packets form a front that has no choice but to explode in the direction normal to the wall. The projection of this front onto the wall encircles the spheroid, and is the logical generalization of the separation point for two-dimensional flows. It unequivocally defines the "separation line" for unsteady three-dimensional separation.

The singular behavior of the boundary-layer at separation is also seen from the continuously increasing $\partial\tilde{u}/\partial\tilde{x}$ near separation. According to the two-dimensional Lagrangian computation of van Dommelen [18], $\partial\tilde{u}/\partial\tilde{x}$ should blow up at separation. Moreover, the velocity profile near separation should exhibit a very "flat" front corresponding to a large inviscid region that splits the boundary-layer into two vorticity layers. The present Eulerian calculation did find a thickening of some velocity profiles as was shown in Fig.9, but none of the profiles are very "flat". Now, given a grid size, a simple estimation based on the Taylor series expansion would suggest an

upper bound of the value $\partial\tilde{u}/\partial\tilde{x}$ that can be determined by differencing. Specifically, when the term $(\Delta\tilde{u}/\Delta\tilde{x})(\Delta\tilde{x})$ becomes order 1, the finite difference formula ceases to be meaningful. In other words, if the mesh $\Delta\tilde{x}$=0.007, which was the grid size near separation in this case, the maximum $\Delta\tilde{u}/\Delta\tilde{x}$ we can get is roughly 150. Indeed in the calculation, it is found that the maximum value of $\Delta\tilde{u}/\Delta\tilde{x}$ hardly exceeded this order. As such a maximum is reached, the singularity is smeared out by the numerical diffusion, and the legitimacy of continuing the calculation becomes questionable. Higher resolution thus is needed to obtain more accurate velocity profiles near separation. Further discussion about this will be given in the subsequent sections.

6° Incidence

This can be considered as an axisymmetry flow perturbed by a small angle of attack. It is expected that most of the features will be similar to those in the 0° incidence. Figure 10 shows the lee-side skin friction, also superimposed is the result by Xu and Wang [15]. The two results do agree in the general trend but not in the values. The skin friction in the tail region is plotted in Fig.11 where details of a small region of reversed flow near the trailing edge are revealed. (This was not available in [15].) Again, no anomalous phenomenon is found in the wall shear, and the whole picture looks almost the same with the one in the previous case (Fig.4) except now the rear stagnation point has shifted upstream a little bit from the rear end. In the present numerical scheme, the velocity profile at the stagnation point is not needed to construct the flow as normally done in a space-marching technique. The stagnation flow evolves by itself. From Fig.11, it is seen that both the stagnation point and the asymmetry of the flow due to the small angle of attack are well captured in the calculation.

Figure 12 exhibits a non-zero distribution of crosswise skin friction $\tau_{y,y}$ at lee-side. At small times, $\tau_{y,y}$ remains negative which indicates that the circumferential velocity v near the symmetry plane is pointing toward the plane of symmetry. As time increases, a region of positive $\tau_{y,y}$ begins to develop near the trailing edge. In other words, a small crosswise reversed flow is formed at the rear end. This reversed flow region will then extend gradually toward the leading edge direction with increasing time. The present results are consistent with those described in [15].

Both the lee-side and wind-side displacement thicknesses in the tail region are shown in Figs.13 and 14. (Details of the displacement thickness near the rear end were left out in Xu and Wang [15], therefore no comparison is made.) By examining Fig.13, it is observed that a "spike" appears first in the wind-side displacement thickness at t=0.25. If we accept the assumption that the initial separation does not substantially alter the flow over the lee-side and simply proceed with the calculation, a similar "spike"-like structure is also found to occur on the lee-side at a somewhat later time (Fig.14). Without the benefit of off-symmetry-plane solution, it may be conjectured here that the separation is likely to occur first as a point on the wind-side symmetry plane and then expand with increasing time in both circumferential directions, and finally, meet on the lee-side symmetry plane to form a closed curve. Turning to the Lagrangian interpretation, because of the presence of a small incidence, fluid "packets" on each different meridian plane will now deform differently. The time at which these "packets" might get squeezed into zero thickness would also differ. Besides, the three-dimensional geometry offers the fluid "packets" a chance to expand in the crosswise direction. The details of how the separation, after its initiation from the wind-side symmetry plane, propagates along the circumferential direction is a question that can only be answered after a fully three-dimensional calculation over the entire prolate spheroid is made.

50° Incidence

After the impulsive start-up, the lee-side skin friction decreases from a maximum value at the leading edge to zero at the rear stagnation point (Fig.15). However, beginning from t=0.05, a dip near the front end is found, and the value of τ_x at the dip drops quickly thereafter. According to the large time calculation of Xu and Wang [15], this value will eventually become negative as a small recirculating bubble is established. A similar situation was found in a high-incidence elliptic cylinder [35] where a reversed flow appears at early time near the leading edge. The skin friction in the tail region is presented in Fig.16. In this picture, the rear stagnation point is located at $\tilde{x}$=-0.23. By the definition of the coordinate transformation, positive $\tilde{x}$ points to wind-side direction. Therefore, positive wall shear around $\tilde{x}$=0 in this plot actually corresponds to a recirculating flow near the rear end. The recirculation region first occurs just shortly above the trailing edge and then expand in both directions. The zero $\tilde{\tau}_{\tilde{x}}$ point moving toward the wind-side direction appears to stop at $\tilde{x}$=0.01, and the recirculation region does not penetrate further upstream. In fact, the skin friction at the wind-side seems to have already reached a steady value at t=0.12. The same trend was also found in the previous two-dimensional calculation [35].

An interesting behavior in the lee-side crosswise skin friction is demonstrated in Fig.17. The reversal of circumferential velocity v (positive $\tau_{y,y}$) first occurs at the rear end and the zero $\tau_{y,y}$ point quickly moves upstream. At t=0.08, another region of reversed v appears at the front and grows in the downstream direction. These two regions coalesce at approximately t=0.12 which means the flow near the symmetry plane is moving away from the plane over the entire lee-side except for a small part close to the leading edge. It is believed that the reversal of the crosswise velocity v will have an important influence on the off-symmetry-plane separation.

At such a high angle of attack, the lee-side displacement thickness at small time still remains essentially constant along most part of the body (Fig.18). Yet a "hump" resulting from the "dip" in the skin friction (Fig.15) is evolved at t=0.05. Near the rear end, the displacement thickness shows a sharp increase and forms a "spike" almost right at the trailing edge (Fig.19). This fact suggests a possible difficulty of the method used by Xu and Wang [15] in obtaining accurate results near the trailing edge, because they did not remove the geometrical singularity there. The reason that the "spike" at t=0.12 appears to be sharper than those presented in the previous cases of this paper is due to a somewhat higher resolution in the present case. The grid size $\Delta\tilde{x}$ near the trailing edge here is approximately 0.001. According to the argument stated at the end of the first subsection, the maximum $\Delta\tilde{u}/\Delta\tilde{x}$ that can be obtained here is around 1000, which is an order larger than that in the zero incidence case. Associated with this result is a "flatter" velocity profile near separation (Figs.20a, b). Although the relevant profiles are not too smooth, the trend is clear. Shown in Fig.21 is one of the corresponding vorticity profiles. The splitting of the boundary-layer into two vorticity layers is apparent.

The calculation was terminated at t=0.12 after the presence of a singularity on the wind-side. Whether or not another singularity may appear at the lee-side near the leading edge can not be answered at this moment. However, suggested by the large time calculation of Xu and Wang [15] and the former results on the elliptic cylinder [35], it is likely that another singularity would develop at later time near the front end, and afterwards the separation would probably be of the "closed" type at this high incidence.

Comparison with Two-Dimensional Results

The results of an unsteady boundary-layer over an impulsively started elliptic cylinder with axes ratio 1/4, calculated by the Lagrangian method described in [35], are presented here for comparison. Shown in Figs.22a, b, c are the displacement thicknesses at 0°, 6° and 50° incidence. In these plots, the time t has been converted to conform with the present time scale. ξ denotes the streamwise boundary-layer coordinate measured along the body from the leading edge in the clockwise direction. Resemblance between the two cases is clear (cf. Figs.8, 14, 19) except that in the Lagrangian result, the "spike" is steeper and more pronounced. This is caused from the high resolution of the Lagrangian grid near separation (p.15). Besides, the displacement thickness in the Lagrangian calculation is obtained from integrating the continuity equation which turns singular

as the separation is approached.

It is noticed that for all three incidences calculated here, separation occurs earlier in time in the two-dimensional case. This can be attributed to the curvature effect as well as the non-zero crosswise velocity v_y in the present three-dimensional calculation.

Figure 23 plots the maximum $\partial\tilde{u}/(\tilde{h}\partial\tilde{x})$ in the present symmetry plane calculation against (t_s-t), t_s being the separation time when the solution turns singular. At t_s, the maximum $\partial\tilde{u}/(\tilde{h}\partial\tilde{x})$ goes to infinity theoretically. We obtain an approximate t_s by extrapolating the zero point of $1/(\partial\tilde{u}/(\tilde{h}\partial\tilde{x}))$ from the available data. In the 50^o incidence case, least-square fittings with models from quadratic to 5^{th} order polynomial give almost the same value of t_s around 0.123. The result for the 6^o incidence is less certain because of the scattering and relatively low value of maximum $\partial\tilde{u}/(\tilde{h}\partial\tilde{x})$, only a quadratic polynomial was used to obtain t_s. Also shown in Fig.28 are the straightlines of slope -7/4 predicted by van Dommelen [18] from the asymptotic structure of the two-dimensional singularity. The dotted line indicates the limiting value of $\partial\tilde{u}/(\tilde{h}\partial\tilde{x})$ beyond which the calculated result is unreliable. The blow-up of maximum $\partial\tilde{u}/(\tilde{h}\partial\tilde{x})$ appears to follow the 7/4 line. This suggests that the structure of the separation on the symmetry plane is similar to that for the two-dimensional case.

SUMMARY

The subject of unsteady three-dimensional boundary-layer separation is of growing importance. Recent understanding about the unsteady separation mechanism reveals that the usual wall shear and limiting streamlines analysis are not strictly applicable to the separation in an unsteady flow. An accurate and efficient computation scheme for a general three-dimensional boundary-layer flow is needed. The present paper is a progress report of a broader research program for this difficult problem.

We propose a non-iterative, time-advancing numerical scheme along with a multiple-zone strategy to solve the unsteady three-dimensional boundary-layer equations. As a preliminary study, the problem of Xu and Wang [15], i.e. the symmetry-plane solution of an impulsively started prolate spheroid with axes ratio 1/4 has been redone. Three different incidences 0^o, 6^o and 50^o are calculated. Results from the examples indicate that the algorithm produce accurate results over the entire symmetrical plane, including certain Lagrangian features near separation found in the two-dimensional case. For the 0^o incidence, projection of the separation locus off the wall on the body necessarily forms a closed curve encircling the spheroid owing to the axisymmetry. For non-zero incidence, separation could conceivably start as a point on the wind-side symmetry plane and then propagate toward the lee-side in the crossflow directions. Whether or not the curve will become closed on reaching the lee-side symmetry plane may depend on the angle of attack. Based on the behavior of the maximum $\partial\tilde{u}/(\tilde{h}\partial\tilde{x})$, the structure of the three-dimensional singularity on the symmetry plane seems to be similar to that for the two-dimensional case.

By using the time-advancing scheme and a flow dependent one-sided spatial difference, the CFL condition is automatically satisfied. No instability was experienced in the calculations. The accuracy of the solution near separation is found to be limited by the requirement of increasing spatial resolution, not by the stability consideration as was inherent in a space-marching technique. Besides, the present time-advancing scheme allows more general flow motions to be calculated while the conventional space-marching scheme has the difficulty of defining a starting profile to initiate the spatial integration.

The primary concern of adopting a multi-zone approach here is to remove the geometrical singularity presented on the prolate spheroid. Since the calculation task in each region is essentially independent, possible implementation of a parallel processing on these multiple regions is therefore worth studying.

ACKNOWLEDGEMENT

Preparation of this work has been partially supported by AFOSR-88-0229. The numerical calculation was performed by using the Cornell National Supercomputer Facility, a resource of the Center for Theory and Simulation in Science and Engineering (Theory Center), which receives major funding from the National Science Foundation and IBM Corporation, with additional support from New York State and members of the Corporate Research Institute.

REFERENCES

1. Lighthill, M. J., In *Laminar Boundary Layers*, ed. L. Rosenhead, Ch.2, Oxford University Press, 1963.
2. Maskell, E. C., "Flow Separation in Three Dimension", RAE Rep. Aero. 2565, 1955.
3. Werle, H., "Separation on Axisymmetrical Bodies at Low Speed", *La Recherche Aeronautique*, Vol., 90, 1962, pp. 3-14.
4. Chanetz, B., "Experimental Investigation of Three-Dimensional Separation on Ellipsoid Bodies at Incidence", IUTAM Symposium on Boundary-Layer Separation, ed. F. T. Smith and S. N. Brown, 1986.
5. Perry, A. E., and Chong, M. S., "A Series-Expansion Study of the Navier-Stokes Equations with Application to Three-Dimensional Separation Patterns", *J. Fluid Mech.*, Vol. 173, 1986, pp. 207-223.
6. Wang, K. C., "Three-Dimensional Boundary Layer Near the Plane of Symmetry of a Spheroid at Incidence", *J. Fluid Mech.*, Vol. 43, 1970, pp. 187-209.
7. Wang, K. C., "Boundary Layer Over a Blunt Body at High Incidence With an Open-Type of Separation", *Proc. Roy. Soc. Lond. Ser. A.*, Vol. 340, 1974, pp. 33-55.
8. Wang, K. C., "Boundary Layer Over a Blunt Body at Low Incidence With Circumferential Reversed Flow", *J. Fluid Mech.*, Vol, 72, 1975, pp. 49-65.
9. Cebeci, T., Khattab, A. A., and Stewartson, K., "Prediction of Three Dimensional Laminar and Turbulent Boundary Layers on Bodies of Revolution at High Angles of Attack", presented at Second International Symposium on Turbulent Shear Flows, 1979.
10. Cebeci, T., Khattab, A. A., and Stewartson, K., "Three-Dimensional Laminar Boundary Layers and OK of Accessibility", *J. Fluid Mech.*, Vol. 107, 1981, pp. 57-87.
11. Cebeci, T., and Su, W., "Separation of Three-Dimensional Laminar Boundary Layers on a Prolate Spheroid", *J. Fluid Mech.*, Vol. 191, 1988, pp. 47-77.
12. Wang, K. C., "Separation Patterns of Boundary Layer over an Inclined Body of Revolution", *AIAA J.*, Vol. 10, 1972, pp. 1044-1050.
13. Wang, K. C., "Laminar Boundary Layer over a Body of Revolution at Extremely High Incidence", *Physics of Fluid*, Vol.17, 1974, pp. 1381-1385.
14. Wang, K. C., "Laminar Boundary Layer near the Symmetry Plane of a Prolate Spheroid", *AIAA J.*, Vol. 12, 1974, pp. 949-958.
15. Xu, W. C., and Wang, K. C., "Unsteady Laminar Boundary Layer Along the Symmetry Plane of an Impulsively Started Prolate Spheroid", *J. Fluid Mech.*, Vol. 195, 1988, pp. 413-435.
16. Ragab, S. A., "The Laminar Boundary Layer on a Prolate Spheroid Started Impulsively from Rest at High Incidence", AIAA-86-1109, 1986.
17. van Dommelen, L. L., and Shen, S. F., "The Spontaneous Generation of the Singularity in a Separating Laminar Boundary Layer", *J. Comp. Phy.*, Vol. 38, 1980, pp. 125-140.
18. van Dommelen, L. L., "Unsteady Boundary-Layer Separation", PhD. Thesis, Cornell University, 1981.
19. Cowley, S. J., "Computer Extension and Analytic Continuation of Blasius' Expansion for Impulsively Flow Past a Circular Cylinder", *J. Fluid Mech.*, Vol. 135, 1983, pp. 389-405.
20. Ingham, D. B., "Unsteady Separation", *J. Comp. Phy.*, Vol. 53, 1984, pp. 90-99.
21. Shen, S. F., "Unsteady Separation of Three-Dimensional Boundary Layers from the Lagrangian Viewpoint" in *Nonsteady Fluid Dynamics*, eds. D. E. Crow and J. A. Miller, ASME, 1978, pp. 47-51.

22. van Dommelen, L. L., and Cowley, S. J., "On the Lagrangian Description of Unsteady Boundary-Layer Separation. Part I : General Theory", to appear in *J. Fluid Mech.*, 1990.
23. Cebeci, T., Khattab, A. A., and Stewartson, K., "On Nose Separation", *J. Fluid Mech.*, Vol. 97, 1980, pp. 435-454.
24. Cebeci, T., "Unsteady Boundary Layers with an Intelligent Numerical Scheme", *J. Fluid Mech.*, Vol. 163, 1986, pp. 129-140.
25. Chesshire, G., and Henshaw, W. D., "Composite Overlapping Meshes for the Solution of Partial Differential Equations", IBM Research Report, RC 14355, 1989.
26. Rai, M. M., "Navier-Stokes Simulation of Rotor/Stator Interaction Using Patched and Overlaid Grids", *J. Prop.*, Vol. 3, 1987, pp. 387-396.
27. Atta, E. H., and Vadyak, J., "A Grid Interfacing Zonal Algorithm for Three Dimensional Transonic Flows About Aircraft Configurations", AIAA-82-1017, 1982.
28. Flores, J., Holst, T. L., Kaynak, U., Gundy, K., and Thomas, S. D., "Transonic Navier-Stokes Wing Solution Using A Zonal Approach : Part 1. Solution Methodology and Code Validation", AGARD-CP-412, paper no. 30A, 1986.
29. Benek, J. A., Buning, P. G., and Steger, J. L., "A 3-D Chimera Grid Embedding Technique", AIAA-85-1523, 1985.
30. Allmaras, S. R., and Baron, J. R., "Embedded Mesh Solutions of the 2-D Euler Equations : Evaluation of Interface Formulations", AIAA-86-0509, 1986.
31. Schmatz, M. A., and Hirschel, E. H., "Zonal Solutions for Airfoil Using Euler, Boundary-Layer and Navier-Stokes Equations", AGARD-CP-412, paper no. 20, 1986.
32. Van Dalsem, W. R., and Steger, J. L., "Efficient Simulation of Separated Three-Dimensional Viscous Flows Using the Boundary-Layer Equations", *AIAA J.*, Vol. 25, 1987, pp. 395-400.
33. Douglas, J., and Jones, B. F., "On Predictor-Corrector Methods for Non Linear Parabolic Differential Equations", *SIAM J.*, Vol. 11, 1963, pp. 195-204.
34. Warming, R. F., and Beam, R. M., "On the Construction and Application of Implicit Factored Schemes for Conservation Laws", *SIAM-AMS Proceedings*, Vol. 11, 1978, pp. 85-125.
35. Wu, T., "Unsteady Incompressible Boundary-Layer Separation Over a Two Dimensional Impulsively Started Elliptic Cylinder Calculated by Lagrangian Method", MS Thesis, Cornell University, 1985.
36. Cebeci, T., "Unsteady Separation", in *Numerical and Physical Aspects of Aerodynamic Flows*, ed. T. Cebeci, 1982, Springer-Verlag.
37. Wang, K. C., "On the Current Controversy about Unsteady Separation", in *Numerical and Physical Aspects of Aerodynamic Flows*, ed. T. Cebeci, 1982, Springer-Verlag.
38. Henkes, R. A. W. M., and Veldman, A. E. P., "On the Breakdown of the Steady and Unsteady Interacting Boundary-Layer Description", *J. Fluid Mech.*, Vol. 179, 1987, pp. 513-529.
39. Kim, J-S, and Chang K-S, "Unsteady Boundary Layer and Its Separation over a Heated Circular Cylinder", *Int. J. Num. Methods in Fluids*, Vol. 8, 1988, pp. 165-179.
40. Shen, S. F., and Wu, T., "Unsteady Separation Over Maneuvering Bodies", AIAA paper no. 88-3542, 1988.
41. Howarth, L., "The Boundary Layer in Three Dimensional Flow - Part 2. The Flow near a Stagnation Point", Phil. Mag., Ser. 7, Vol. 42, no. 335, 1951, pp. 1433-1440.

APPENDIX

In this appendix, accuracy of the present numerical calculations is estimated by studying the effect of grid refinement on the value of skin friction at the front stagnation point. On the stagnation line, the velocity component u is identically zero. The derivative of the skin friction at stagnation is obtained by

$$\tilde{\tau}_o = (\tilde{\tau}_{\tilde{x},\tilde{x}} / \tilde{h}) / (\tilde{U}_{e,\tilde{x}} / \tilde{h})^{3/2}.$$

The scaling factor $(\tilde{U}_{e,\tilde{x}} / \tilde{h})^{3/2}$ is introduced here for the purpose of comparison with Howarth's steady state result [41]. At steady state, $\tilde{\tau}_o$ is equivalent to f"(0) defined in [41]. For the axisymmetrical case, f"(0)=1.312.

Table 1 lists $\tilde{\tau}_o$ at t=0.2 calculated at three different mesh sizes with time step Δt equals 0.02, 0.01 and 0.005 respectively. All three values appear to approach the steady state result 1.312 given by Howarth. The last row of the table is the Richardson extrapolation of the above three meshes. Using this value as a reference "exact" solution, errors in $\tilde{\tau}_o$ obtained from each grid size are listed in the second column. Convergence of the result is apparent.

Table 1. Effects of grid refinement on the value of skin friction at stagnation point.

grid size	$\tilde{\tau}_o$	error
30 x 31	1.310660	0.001269
60 x 61	1.311750	0.000179
120 x 121	1.311893	0.000036
RE	1.311929	- - -

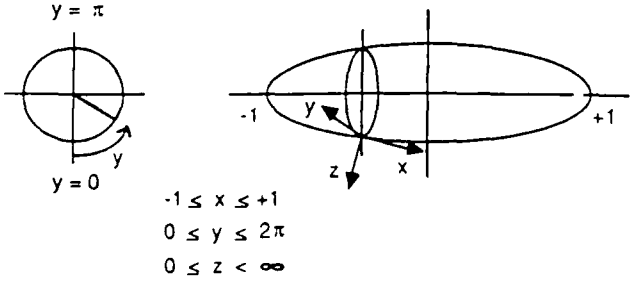

Fig.1 Geometry and coordinates system.

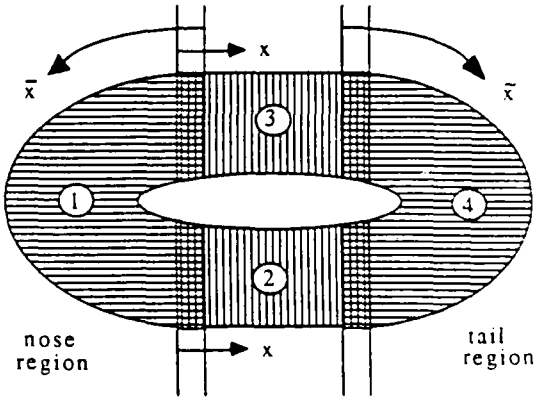

Fig.2 Multiple zones.

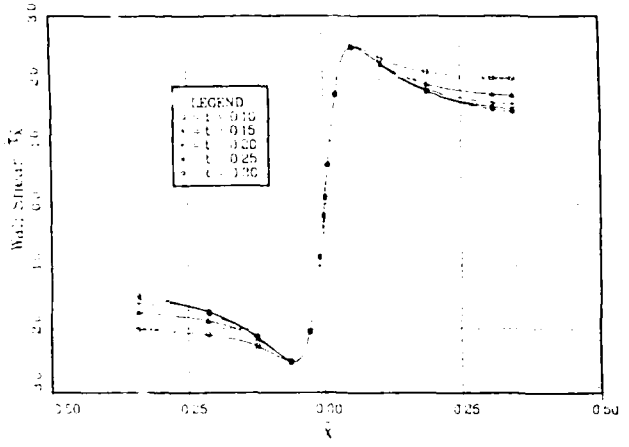

Fig.3 Skin friction $\tilde{\tau}_{\tilde{x}}$ in nose region ($\hat{\alpha} = 0^{o}$).

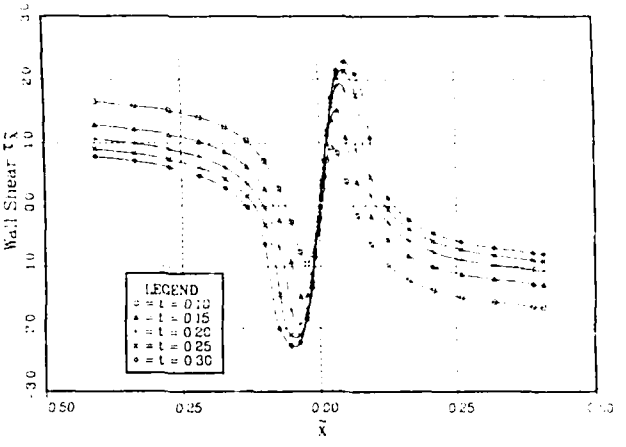

Fig.4 Skin friction $\tilde{\tau}_{\tilde{x}}$ in tail region ($\hat{\alpha} = 0^{o}$).

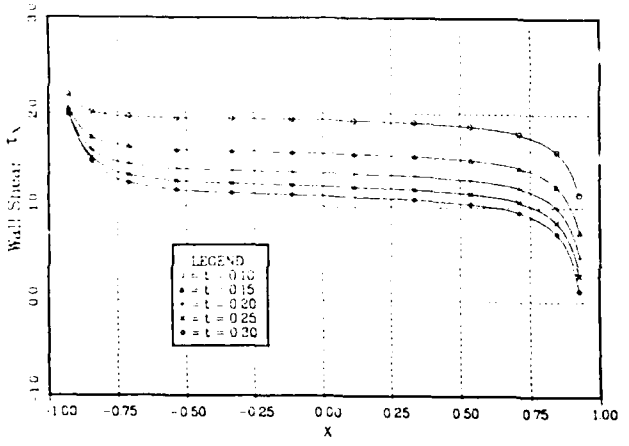

Fig.5 Lee-side skin friction τ_x ($\hat{\alpha} = 0^{o}$).

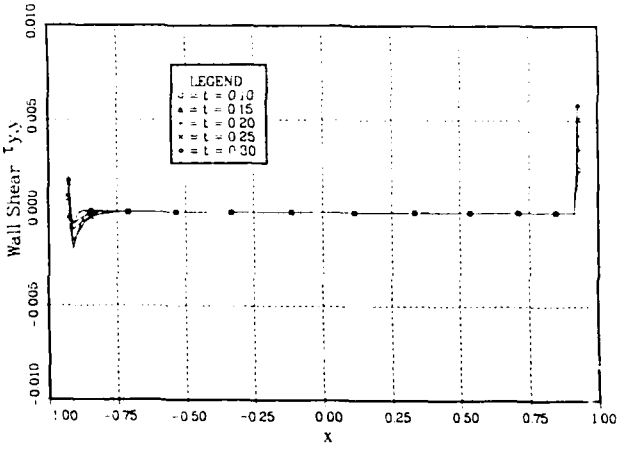

Fig.6 Lee-side crosswise skin friction $\tau_{y,y}$ ($\hat{\alpha} = 0^{o}$).

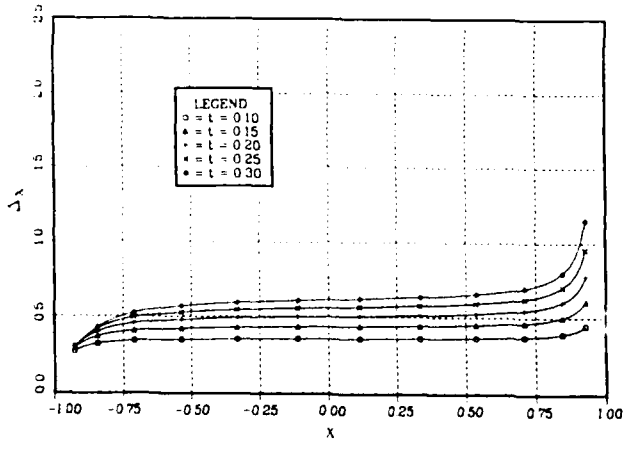

Fig.7 Lee-side displacement thickness Δ_x ($\hat{\alpha} = 0^{o}$).

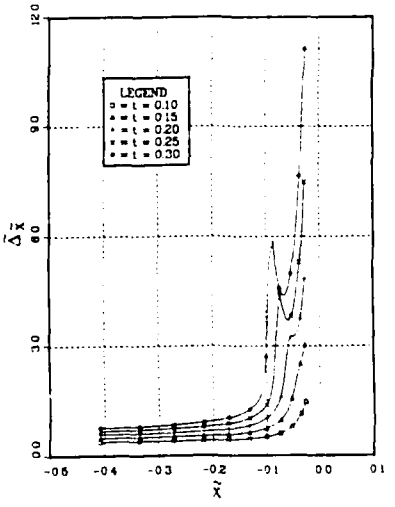

Fig.8 Displacement thickness $\tilde{\Delta}_{\tilde{x}}$ in tail region ($\hat{\alpha} = 0^{o}$).

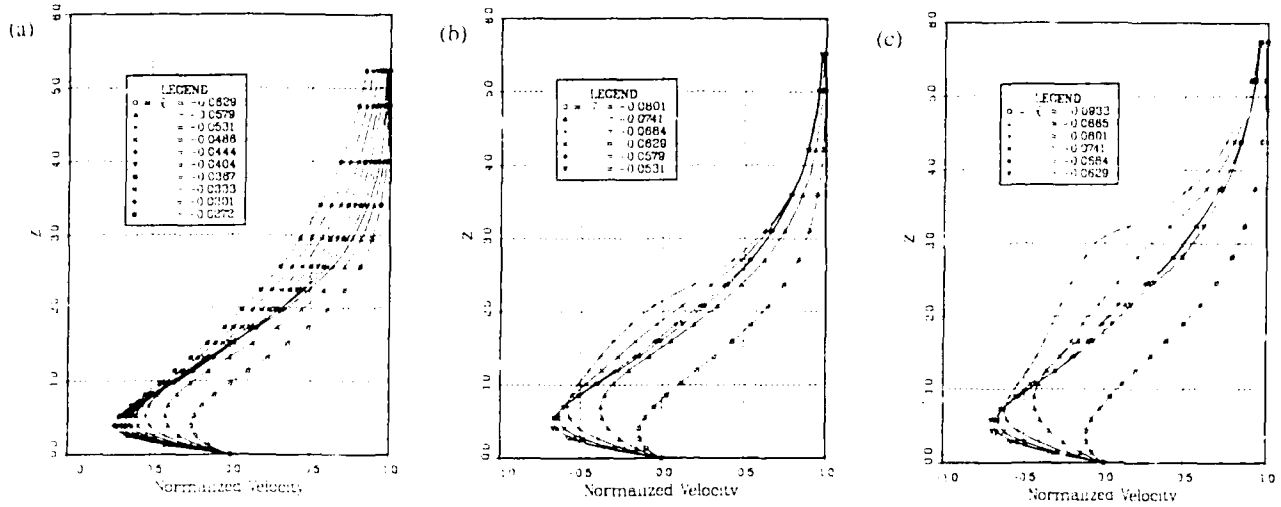

Fig.9 Velocity profiles at $\hat{\alpha} = 0^{o}$; (a) t = 0.19, (b) t = 0.23, (c) t = 0.27.

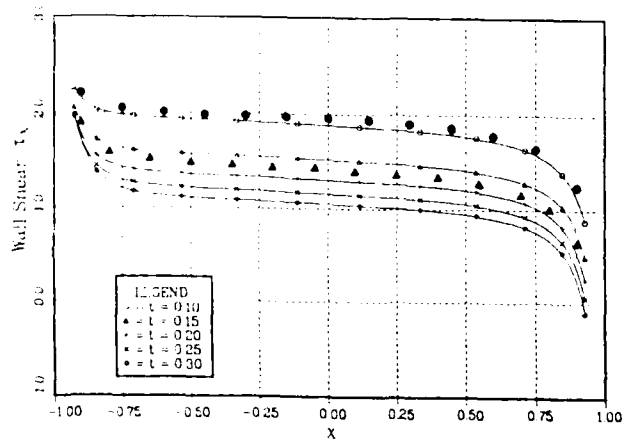

Fig.10 Lee-side skin friction τ_x ($\hat{\alpha} = 6^{o}$); ● - t = 0.1, ▲- t = 0.2, Xu and Wang [15].

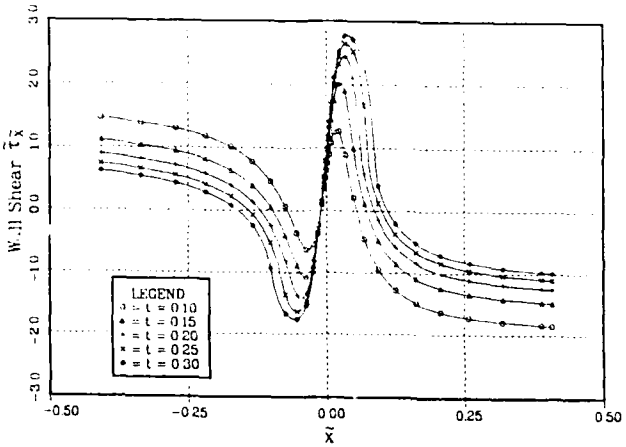

Fig.11 Skin friction $\tilde{\tau}_{\tilde{x}}$ in tail region ($\hat{\alpha} = 6^{o}$).

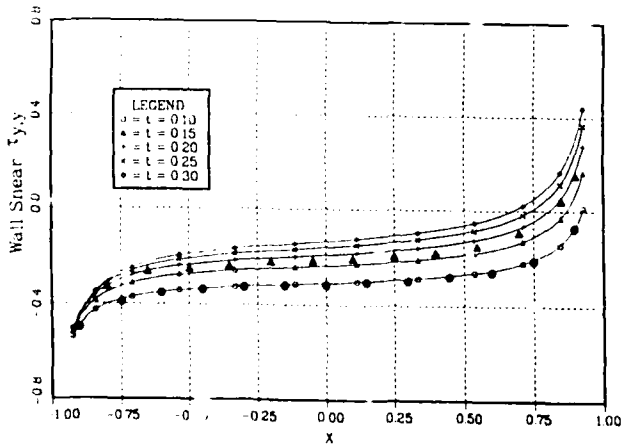

Fig.12 Lee-side crosswise skin friction $\tau_{y,y}$ ($\hat{\alpha} = 6^{o}$); ● - t = 0.1, ▲ - t = 0.2, Xu and Wang [15].

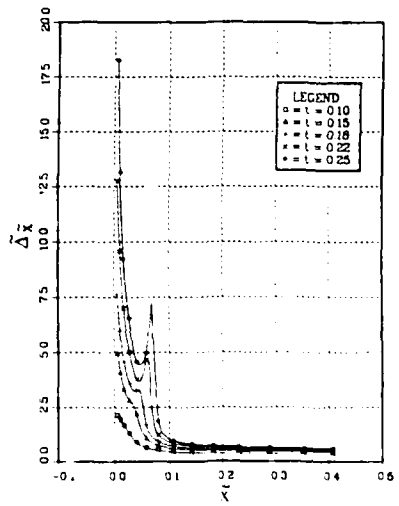

Fig.13 Displacement thickness $\tilde{\Delta}_{\tilde{x}}$ in tail region, wind-side ($\hat{\alpha} = 6^{o}$).

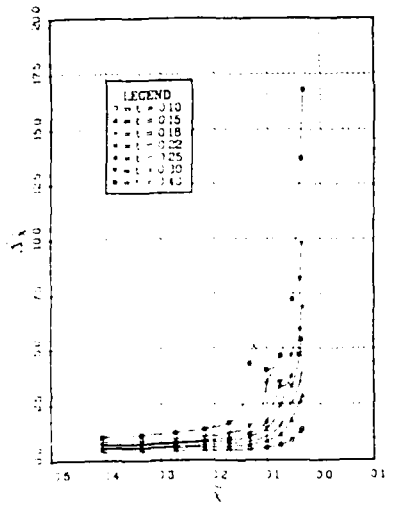

Fig.14 Displacement thickness $\tilde{\Delta}_{\tilde{x}}$ in tail region, lee-side ($\hat{\alpha} = 6^{o}$).

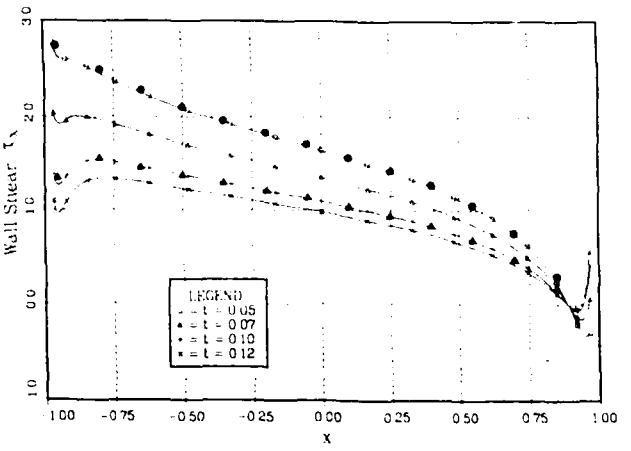

Fig.15 Lee-side skin friction τ_x ($\hat{\alpha} = 50^{o}$); ● - t = 0.05, ▲- t = 0.1, Xu and Wang [15].

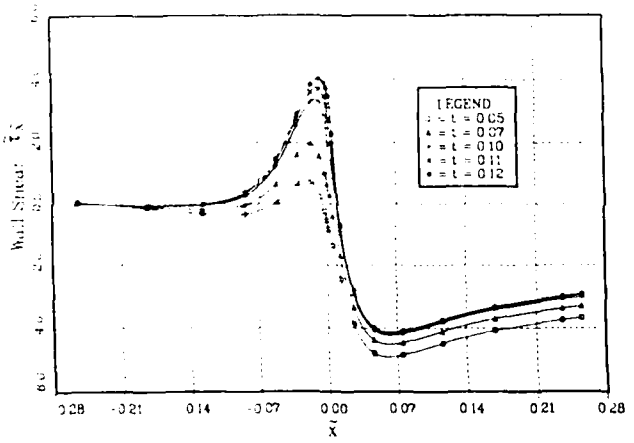

Fig.16 Skin friction $\tilde{\tau}_{\tilde{x}}$ in tail region ($\hat{\alpha} = 50^{o}$).

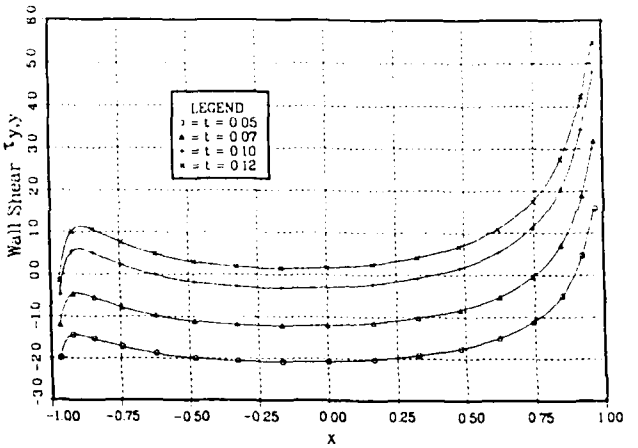

Fig.17 Lee-side crosswise skin friction $\tau_{y,y}$ ($\hat{\alpha} = 50^{o}$).

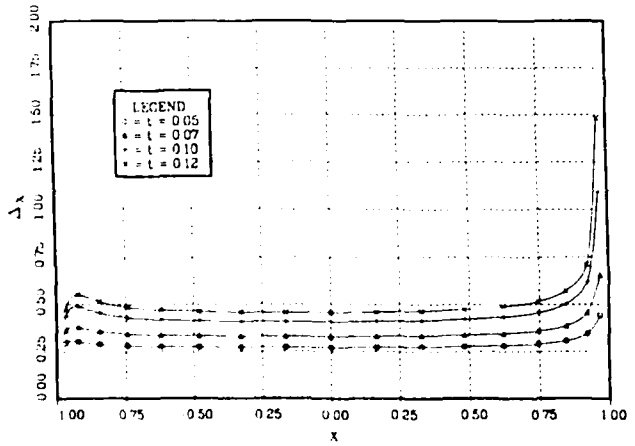

Fig.18 Lee-side displacement thickness Δ_x ($\hat{\alpha} = 50^{o}$).

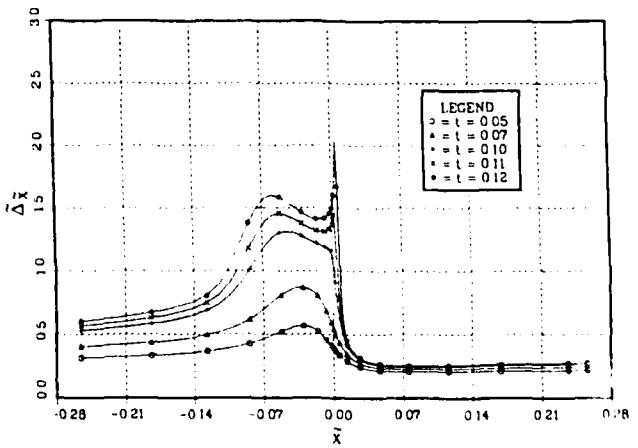

Fig.19 Displacement thickness $\tilde{\Delta}_{\tilde{x}}$ in tail region ($\hat{\alpha} = 50^{o}$).

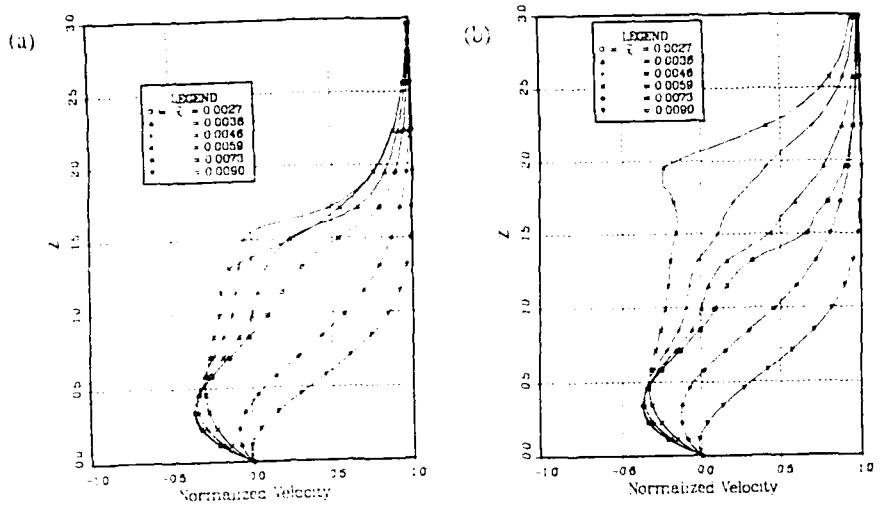

Fig.20 Velocity profiles at $\hat{\alpha} = 50^{o}$; (a) t = 0.12, (b) t = 0.122.

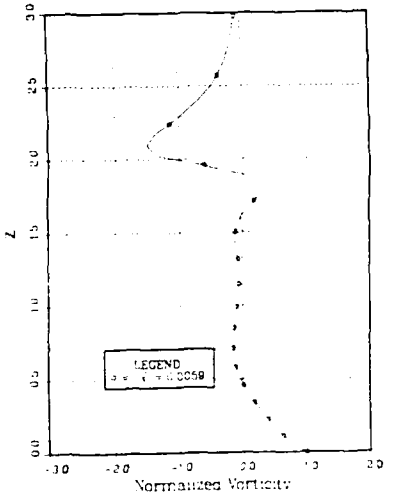

Fig.21 Vorticity profile near separation. t = 0.122 ($\hat{\alpha} = 50^{o}$).

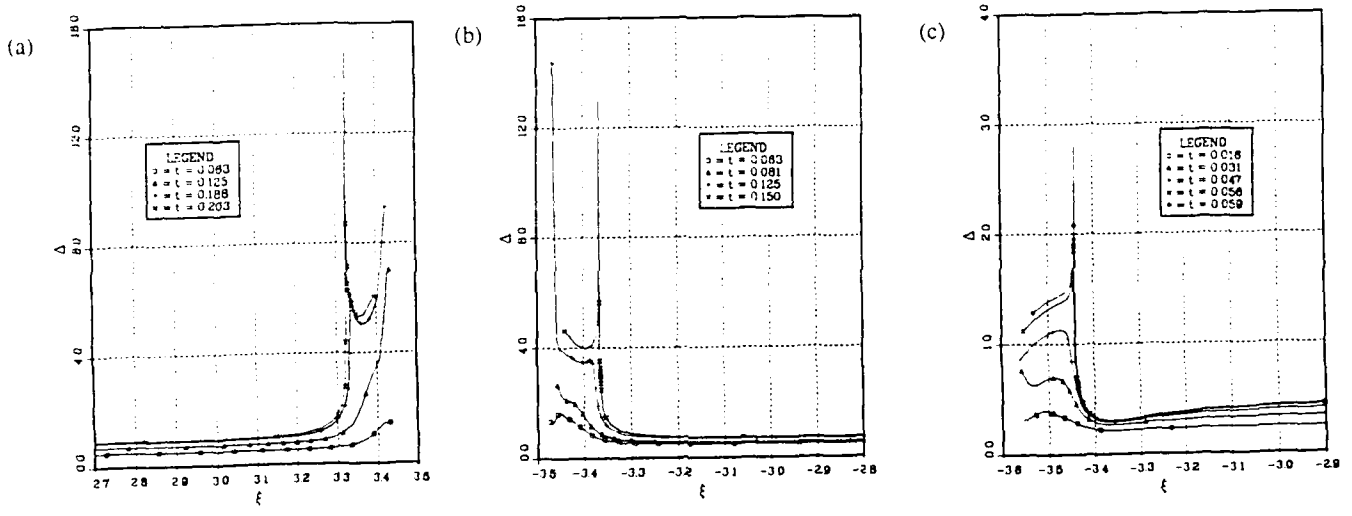

Fig.22 Displacement thickness of an impulsively started elliptic cylinder calculated by the Lagrangian method; (a) $\hat{\alpha} = 0^{o}$, (b) $\hat{\alpha} = 6^{o}$, (c) $\hat{\alpha} = 50^{o}$.

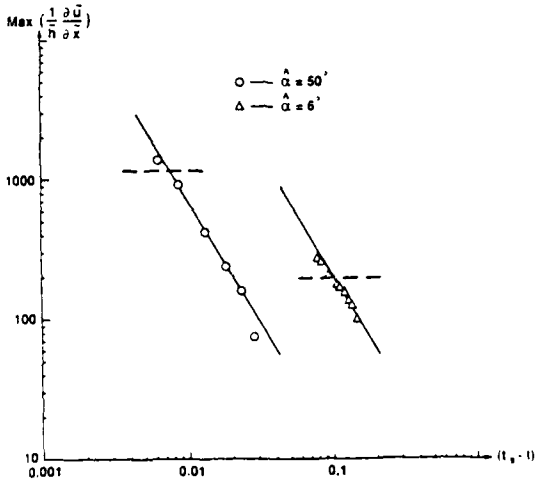

Fig.23 Blow-up of Max $(1/\tilde{h})(\partial\tilde{u}/\partial\tilde{x})$ as calculated by the present Eulerian scheme, —— straight line of 7/4 slope predicted in the two dimensional case.

Appendix B
TR 1229, 2/90

Code Development for the Unsteady Thin-Layer Navier-Stokes Equation Using a Non-Iterative FDM

Jae-Soo Kim

Mar. 1990

I. Introduction

Since the noniterative factorization method for the compressible Navier-Stokes equation was developed by Beam & Warmming(1), several similar noniterative methods have been investigated to solve the compressible and the incompressible flows. In Beam & Warmming(1)'s technique, the governing equation can be noniteratively solved without loss of accuracy. This scheme is a kind of three point backward implicit ADI method developed by McDonald and Briley(2).

But, even though the Navier-Stokes can be solved without iterations, a large amount of computer time and storage is needed to solve any simple flow. Though only the steady solution is needed, the unsteady equation is calculated in time until a steady state solution is achieved. Moreover, it is possible to obtain the accurate solutions of many viscous flows with several reduced sets of equations, such as boundary layer equations, thin-layer, or parabolized Navier-Stokes equations. So, many researchers have developed the noniterative methods to solve the reduced sets of equations.

These noniterative methods, which have been developed on the base of Beam & Warmming's delta scheme, can be divided into two catagories, i. e. one for compressible flows, and another for incompressible flows. Steger(3) used the technique to solve the unsteady thin-layer Navier-Stokes equation. The thin-layer Navier-Stokes equation is considerably less complicated than the complete Navier-Stokes

equation because of the approximation of dropping some viscous terms in the Navier-Stokes equation. But, the procedure of calculation still requires a substantial amount of computer effort to solve three dimensional flows. So, Schiff and Steger(4) developed the noniterative scheme to solve the parabolized Navier-Stokes equation to predict three dimensional, steady, supersonic viscous flowfield. This method requires that the inviscid outer flow must be supersonic and the primary streamwise velocity component must be positive everywhere. But the cross flow separation is permitted. An additional constraint is that the streamwise pressure gradient in the region of subsonic must be handled to neglect the elliptic characteristics of the governing equation.

As above, though many noniterative schemes have been developed and popularly used to solve compressible flows, only a few schemes have been developled for incompressible flows. Kim and Chang(5) used the noniterative technique to solve for unsteady incompressible boundary layers. But, it can not be applied to the flow which includes the region of reverse flow, exept for some spetial cases. Kwak(6) developed the technique to solve the steady incompressible Navier-Stokes equation using the artificial compressibility method of Chorin(7). Although this method used the linearized factorization technique, it is the iterative scheme to obtain steady solutions.

Some iterative methods have been developed to solve the steady parabolized Navier-Stokes equation. The streamwise derivative term of pressure is treated explicitly in these methods. In Patankar and Spalding(9), the pressure in the streamwise momentum equation is assumed to vary only in the streamwise direction. But, the variation of pressure in a cross plane is permitted. Chilukuri and Pletcher(10)

considered the effect of the elliptic characteristic by marching in the streamwise direction in an iterative method. This scheme was originally restricted to flows in which the reverse flow in the primary flow direction doesnot occur. But, Madavan and Pletcher(11) have demonstrated two dimensional flows in which the reverse flow in the primary flow direction occurs. But, all of these methods are iterative methods for steady solutions.

Here, a code is developed to solve the unsteady 3-dimensional thin-layer Navier-Stokes equation by using the noniterative finite difference method. At first, the Navier-Stokes equation written in the general coordinates (ξ,η,ζ) is simplified by the thin-layer approximation, which neglect the viscous terms including the derivatives of the streamwise or the spanwise direction. This thin-layer equation is linearized and factorized by the noniterative technique. The resulting factorized equation is solved by a 3-step block tri-diagonal matrix elimination. The central difference is used to discretize the derivatives of the spanwise and the normal directions, but the central or backward difference is used for the streamwise direction.
The flow which has a leading edge stagnation point can not be solved by the central difference, because the results are unstable between the initial point and the leading edge stagnation point. So, the backward difference is applied to the derivatives of velocities in the momentum equations between the initial point and the leading edge stagnation point. This method helps to stabilize the scheme, but the results are slowly disturbed again from the leading edge stagnation point.

Some numerical examples are investigated, such as the transient development of Couette flow, the flow over a suddenly started finite flat plate, the flow over a suddenly started circular cylinder and the transient flow over a 3-dimensional wave wall.

References

1. Beam and Warmming, "An implicit factorization scheme for the compressible Navier-Stokes equation," AIAA J., vol.16, pp.393-402, 1978.

2. McDonald and Briley, "Three dimensional supersonic flow of a viscous or inviscid gas," J. of Comp. Phys., vol.19, pp.150-178, 1975.

3. Steger, "Implicit finite difference simulation of flow about arbitrary two dimensional geometries," AIAA J., vol.16, pp.676-686, 1978.

4. Schiff and Steger, "Numerical simulation of steady supersonic viscous flow," AIAA J., vol.18, pp.1421-1430, 1980.

5. Kim and Chang, "Unsteady boundary layer and its separation over a heated circular cylinder," Int. J. for Num. methods in Fluids, vol.8, pp.165-177, 1988.

6.Kwak, Chang and Shanks, "A 3-dimensional incom. N-S flow solver using Primitive variables," AIAA J., vol.24, pp.390-396, 1989.

7. Chorin, "Numerical method for solving incompressible viscous flow problems," J. Comp. Phys., vol.2, pp.12-26,1968.

8. Patankar and Spalding, "A calculation procedure for heat, mass and momentum transfer in three dimensional parabolic flows," Int. J. Heat Mass Transfer, vol.15, pp.1787-1806, 1972.

10. Chilukuri and Pletcher, "Numerical solutions of the partially parabolized Navier-Stokes equation for developing flow in a channel," Num. Heat Transfer, vol.3, pp.169-188, 1980.

11. Madavan and Pletcher, "Prediction of incompressible laminar separated flows using the partially parabolized Navier-Stokes equations," Eng. Research Institute Technical Report 82127/HTL-27, Iowa State Univ., Ames, 1982.